



Modification of coconut shell activated carbon and purification of volatile organic waste gas acetone

Zhihua Deng¹ · Qiuhan Zhang² · Qing Deng¹ · Zhanhu Guo³ · Ilwoo Seok⁴ 

Received: 19 April 2021 / Revised: 25 August 2021 / Accepted: 13 September 2021 / Published online: 1 October 2021
© The Author(s), under exclusive licence to Springer Nature Switzerland AG 2021

Abstract

The impregnation method was used to modify the coconut shell activated carbon, and the modified activated carbon was applied to purify the simulated exhaust gas of acetone. The experiment first discussed the influence of modification conditions on activated carbon's adsorption effect and determined the best modification conditions. Specifically, the adsorption operation conditions such as intake time, intake flow rate, intake concentration, and adsorption temperature were investigated. Then, characterization methods such as BET and FTIR were used to study the thermodynamic and kinetic processes of activated carbon's adsorption process by acetone and the in-depth analysis of the purification mechanism. The results show that a 1% KOH modified coconut shell activated carbon has the highest adsorption performance. Both the Langmuir adsorption isotherm model and the Bangham kinetic model can better fit the adsorption process. Experimental outcomes will support the theoretical approach for the research of coconut shell activated carbon in acetone purification.

Keywords Adsorption of thermodynamics · Adsorption of kinetics · Coconut shell-based activated carbon

1 Introduction

The rapid development of the heavy industry and automotive market has caused a sharp rise in emissions of volatile organic compounds such as acetone [1], which negatively affects the environment and health. Acetone is a colorless and transparent liquid with aromatic ether and mint flavors. It is widely used in electroplating production, spray paints, and other spraying products with a low-temperature plasma technology [2], catalytic combustion method [3], and biological

method [4], membrane separation method [5], adsorption method [6, 7], and several other purification methods [8–11]. Activated carbon has been extensively used in acetone adsorption studies due to its large specific surface area, strong adsorption capacity, and low cost [12, 13]. Mao et al. studied the adsorption of toluene and acetone vapor by pine sawdust activated carbon [14]. This research reported that the adsorption capacity of pine sawdust activated carbon for toluene and acetone can reach 0.71 g/g and 0.57 g/g, respectively. Kam et al. used the activated carbon prepared from discarded citrus peels and applied it to adsorb acetone and benzene [15]. It is observed that the adsorption capacity on the target gas increases proportionally to the inlet concentration, the highest being benzene, followed by acetone. Besides, Yang Qunjun et al. [16, 17] obtained polystyrene-based spherical activated carbons (PACSs) by sulfonation, carbonization, and water vapor activation and utilized it to adsorb low concentrations of acetone. Their results show that acetone reaches the maximum adsorption capacity at 1 h of the activation time. All the above studies have proved that modification can significantly improve the adsorption performance of activated carbon.

In this research, the solid wastes of agricultural and forestry products-activated carbons were modified using

✉ Zhihua Deng
dengzhoo@163.com

✉ Ilwoo Seok
iseok@astate.edu

¹ College of Ecology and Environment, Southwest Forestry University, Kunming 650233, China

² College of Chemical Engineering, Southwest Forestry University, Kunming 650233, China

³ Integrated Composites Lab (ICL), Department of Chemical & Biomolecular Engineering, University of Tennessee, Knoxville, TN 37996, USA

⁴ College of Engineering and Computer Science, Arkansas State University, Jonesboro, AR 72467, USA

KOH [18]. The modifier's concentration on the functional group content on the coconut shell's surface activated carbon was investigated. Furthermore, the removal efficiency and adsorption capacity of modified coconut shell activated carbon were studied. The effects of modification conditions and adsorption operation conditions on the purification were investigated, and theoretical support for future research was provided.

2 Materials and methods

2.1 Material preparation of coconut shell-based activated carbon

Reagents such as KOH and acetone were used in the experiment, which were analytically pure. Coconut shell activated carbon, from Gongyi Guoqing Water Purification Material Co., Ltd., and its main physical and chemical properties are shown in Table 1.

2.2 Modification of activated carbon

For the KOH modification process, 1%, 3%, 5%, and 10% KOH solutions were prepared. Then, 50 g of activated carbon (AC) was immersed with a 200-mL KOH solution with a 4:1 solid–liquid ratio. A conical flask containing the modifier and coconut shell activated carbon was placed in a desktop thermostatic vibration box at a speed of 200 rpm. The samples were shaken at 25 °C for 24 h, and the obtained coconut shell activated carbon samples were referred to like 1% KOH-AC, 3% KOH-AC, 5% KOH-AC, and 10% KOH-AC, respectively.

For the adsorption of acetone by coconut shell activated carbon, each experiment weighs 9 g of coconut shell activated carbon and places it into the activated carbon adsorption column with a size of 2 cm and 20 cm for inner diameter and height, respectively. The constant temperature system controlled the adsorption temperature. At the temperature (293 K, 298 K, 303 K), the air intake flow rates (50, 100, 150, 200, 250 mL/min) with intake times (5, 7, 10, 15, 20, 25, 30, 35, 40, 45, 50, 60, 70, 80, 90, 100, 120, 140, 160, 180 min) were tested. A Thermo Scientific High-Performance Liquid Chromatograph (UltiMate 3000) was utilized to measure

the experimental conditions of temperatures, times, and intake flow rates. The sample's content from the intake air — before and after — was analyzed for the removal efficiency and adsorption amount of acetone by coconut shell activated carbon.

For the characterization of modified coconut shell activated carbons, 1 g of activated carbon was placed in 250-mL Erlenmeyer flasks, and 50 mL of 0.05 mol/L HCl of the standard solution was added, sealed in a constant temperature vibration box at 200 rpm, with a temperature of 25 °C for 24 h. After the operation, the mixture was rested for 1 h and filtered to separate the solution from the activated carbon. Twenty-five milliliters of the solution was accurately transferred into a 250-mL conical flask using the pipette. With methyl red as the endpoint indicator, the solution was titrated with 0.05 mol/L NaOH standard solution until the acid solution in the Erlenmeyer flask was neutralized entirely. Calculated as follows:

$$Q = \frac{V_1 - V_2(A/V_2)}{m} \times 0.05$$

where Q is the content of primary functional groups, mmol/g; V_1 is the volume added with 0.05 mol/L HCl in mL; V_2 is the volume of HCl used for sample titration in mL; A is the volume of 0.05 mol/L NaOH consumed for trans titration in mL; m is the mass of activated carbon in gram.

For the characterization of acetone and 1% KOH-AC, a fully automatic three-station specific surface and porosity analyzer (TriStar II 3020) is used to determine high purity nitrogen at 77 K at AC and 1% KOH-AC adsorption and desorption isotherm. Fourier transform infrared spectrometer (Bruker Tensor 27) produced by Bruker Spectroscopy, Germany, was used to determine the functional group types of AC and 1% KOH-AC. one hundred to two hundred milligrams of dry analytical pure KBr with 1–2 mg of sample was placed in an agate mortar and ground into a fine powder with a particle size of less than 2 μm under an infrared lamp and mixed uniformly. Fine ground powder was then placed in a tableting mold and maintained for 3 to 5 min under a pressure of 15 to 20 MPa. Afterward, the powder was scanned at a wavelength of 4000 to 400 cm⁻¹ to obtain an analysis band. This spectral transfer of the band was then used to determine the change of the functional group of the material.

Table 1 The main physical and chemical properties of coconut shell activated carbon

Iodine value, mg/g	strength/%	Methylene blue value, mg/g	Moisture/%	Specific surface area, mg/g	Packing density/%	Ash/%	PH
900~1100	≥90	100~150	≤5	1000	0.45~0.55	≤8~12	8~10

In acetone’s determination process by high-performance liquid chromatography, the chromatographic column is a C18 column with a size of 4.6×250 mm, and an inner diameter of 5 μm was used. The mobile phase of methanol plus water was 50+50 (V/V) and filtered through a 0.45-μm filter membrane. Ultrasonic degassing was processed at the column temperature of 30 °C. Flow rate with 1.0 mL/min, detection wavelength in 254 nm, and injection volume 10 μL were set up, respectively. Under these conditions, the peak position of acetone was about 3.3 min.

3 Results and discussion

3.1 Effect of KOH modification on the adsorption efficiency of coconut shell activated carbon

The activated carbon was modified with KOH solutions of different concentrations, and the acetone removal efficiency of coconut shell activated carbon was observed with time. The results are shown in Fig. 1. KOH-modified coconut shell activated carbons presented a particular ability to remove acetone. One percent of KOH modifier exhibits the best removal effect for a long time, with constant removal efficiency at 100%. The adsorption amount of acetone on KOH-modified coconut shell activated carbon with different mass concentrations was measured and is listed in Table 2.

As shown in Table 2, the adsorption amount of acetone decreases as increasing KOH concentration; the equilibrium adsorption amounts are 0.96, 0.57, 0.56, and 0.50 mg/g. Compared with real coconut shell activated carbon, the adsorption by 1% KOH-modified coconut shell activated carbon marked 136.09 μg/mL, and the equilibrium adsorption capacity reached 0.96 mg/g. Compared to the AC having 0.70 mg/g absorption capacity, the equilibrium adsorption amount increased by 35.69%. The other three modified coconut shell activated carbons (3, 5, 10% KOH-AC) show the reduced adsorption capacity with 18.38%, 20.53%, and 29.37%.

The adsorption capacity of acetone on coconut shell activated carbon modified with different KOH concentrations was tracked over time, as shown in Fig. 2. As the intake airtime increases, the adsorption capacity of modified coconut shell activated carbon for acetone increases first and then saturates at a certain point. It is ordered as 1% KOH-AC > AC > 3% KOH-AC = 5% KOH-AC > 10% KOH-AC. The equilibrium adsorption of acetone by 1% KOH-AC is saturated to the value of 0.96 mg/g as listed in Table 2.

3.2 Effect of KOH modification on the adsorption efficiency of coconut shell activated carbon

Figure 3 shows the microscopic structures of materials of unmodified activated carbon and activated one. The

Fig. 1 Dynamic change of acetone removal efficiency with different concentration of KOH-modified coconut shell activated carbon

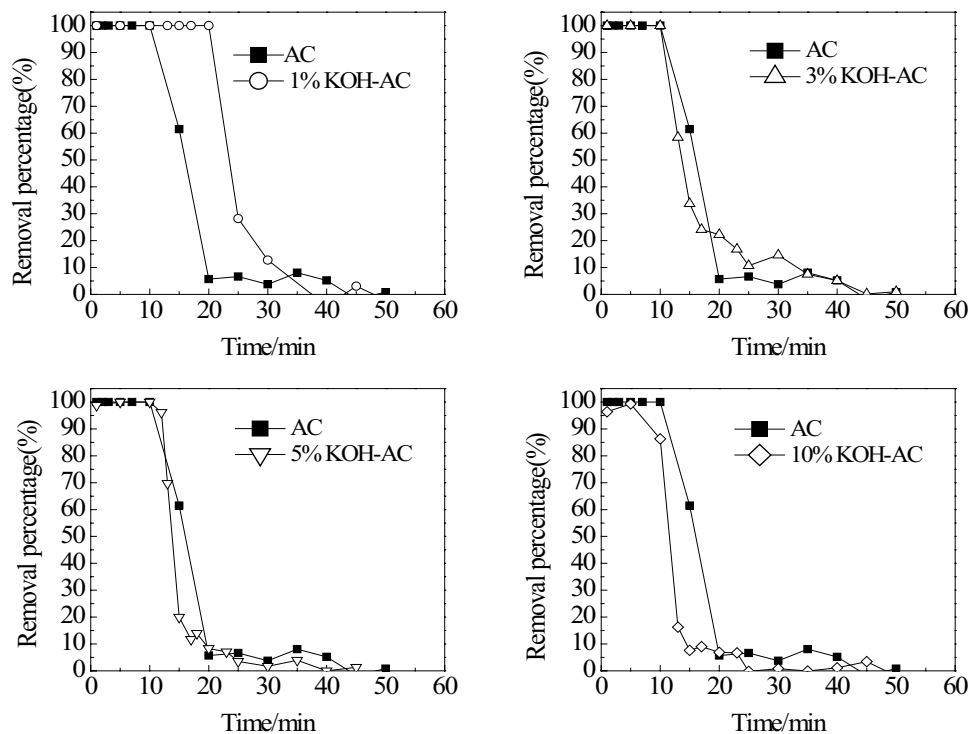


Table 2 Adsorption of acetone by coconut shell activated carbon modified under different concentrations of KOH modifier

Adsorbate	Adsorbent	Equilibrium concentration, $\mu\text{g/mL}$	Equilibrium adsorption capacity, mg/g	Adsorption capacity growth rate (%)
Acetone	AC	145.31	0.70	0
	1% KOH-AC	136.09	0.96	35.69
	3% KOH-AC	122.83	0.57	-18.38
	5% KOH-AC	138.31	0.56	-20.53
	10% KOH-AC	154.03	0.50	-29.37

sample modified by 1% KOH agent shows the difference from the unmodified one. The surface is rougher and more porous. Besides, the pores' distribution is denser, and the pores extend deeply to the organizations inside. This enables modified ones to have larger surface areas. This helps improve the physical and chemical properties of coconut shell activated carbon for target materials' adsorption.

3.3 Characterization of coconut shell activated carbon

The adsorption and desorption isotherms of nitrogen on AC and 1% KOH-AC were measured by the low-temperature nitrogen (77 K, N_2) adsorption and desorption method. The cyclic graph in Fig. 4 shows the results of adsorption capacity in mL/g verse relative pressure on two adsorbents of AC and 1% KOH-AC.

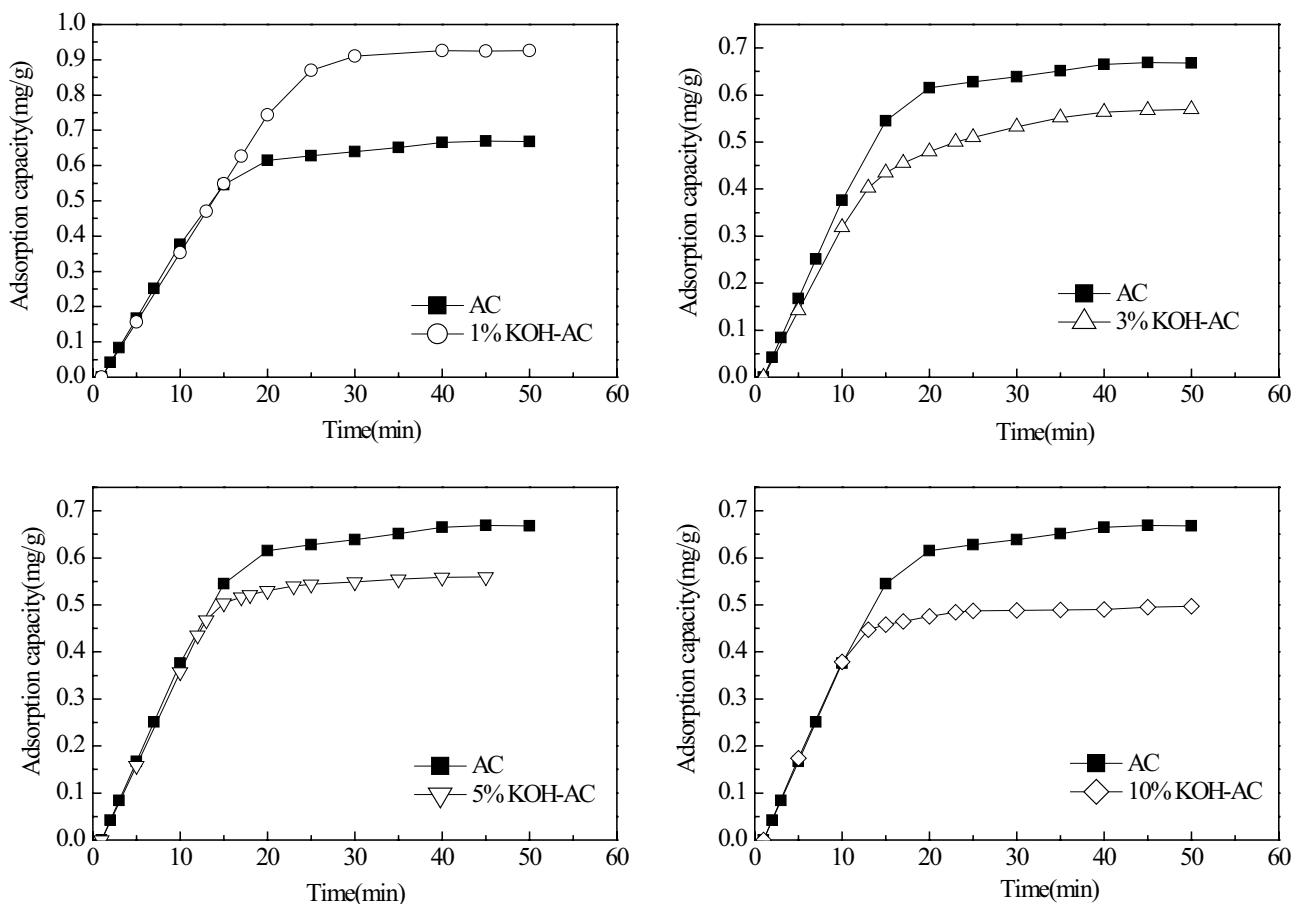
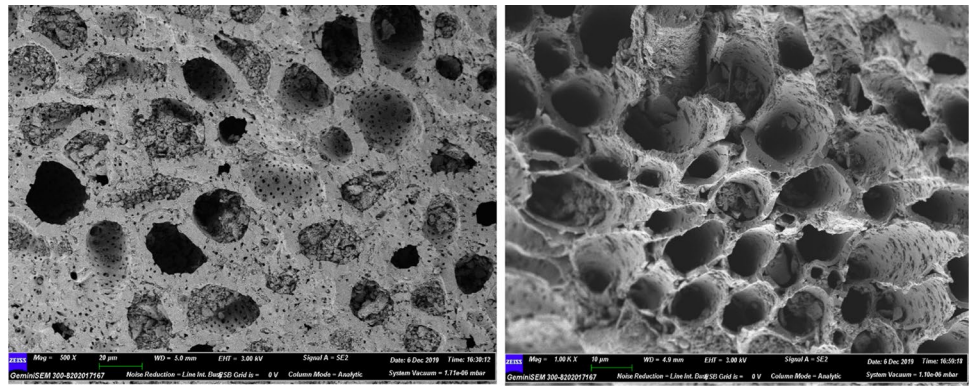
**Fig. 2** The dynamic change of acetone adsorption on coconut shell activated carbon modified with different concentration of KOH

Fig. 3 Scanning electron microscope images of unmodified activated carbon (left) and 1% KOH modified activated carbon (right)



Measured specific surface area and pore volume for adsorbents are listed in Table 3. The pore structures of AC and 1% KOH-AC were calculated from the low-temperature N_2 desorption curve data using the BJH (Barrett, Joyner, and Halenda) method. The corresponding total pore volume V_{total} was calculated using the amount of liquid nitrogen adsorbed at a relative pressure of 0.9814. The pore size distributions are then obtained by analyzing the branch of the isotherm of the low-temperature N_2 adsorption and isotherm based on the BJH method as in Fig. 4.

The adsorption and desorption isothermal curves of AC and 1% KOH-AC have an upward trend with relative pressure. Moreover, based on the BET (Brunauer–Emmett–Teller) surface area analysis, the adsorption mode was classified as type IV.

Lowercase letters are the percentages of micropore, mesopore, and macropore to the total pore volume.

According to Table 3, the order of the BET specific surface area is AC > 1% KOH-AC, and for micropore pore volume: AC > 1% KOH-AC, and for the mesopore pore volume, 1% KOH-AC increased up to the AC. The microporosity and mesoporosity of AC are 46.26% and 40.56%, respectively. The microporosity of 1% KOH-AC with 45.78% is more remarkable than the mesoporosity with 41.51%. Both adsorbents of AC and 1% KOH-AC

showed the developed mesoporous and microporous structures. This mesopore structure impacts the results of N_2 adsorption and desorption isotherm, as shown in Fig. 4.

Figure 5 shows the average pore size for AC and 1% KOH-AC within the mesoporous region. Peaked distribution means that AC and 1% KOH-AC both contain multiple pore structures. The higher the peak, the higher the porosity. One percent KOH-AC has a higher porosity than AC, consistent with the values in Table 3.

3.4 Fourier transform infrared spectrum

Fourier transform infrared spectrum scanning of AC, and 1% KOH-AC was performed, and the results are shown in Fig. 6.

As shown in Fig. 6 (left), the surface of AC and 1% KOH-AC contains some typical functional group bands, which are characteristic peaks of OH at the wavenumber of 3558 cm^{-1} , 1618 cm^{-1} , and 1641 cm^{-1} . The characteristic peaks of NH are all at 3417 cm^{-1} wavenumber, the characteristic peaks of $-\text{NO}_2$ are at 1554 cm^{-1} wave number, and the characteristic peaks of $-\text{CH}_3$ and $-\text{CH}_2$ are at 1456 cm^{-1} wave number. From Fig. 6 (right), 1% KOH-AC has new peaks of OH at 3593, 3450, 3383,

Fig. 4 Nitrogen adsorption–desorption isotherm of coconut shell activated carbon at 77 K

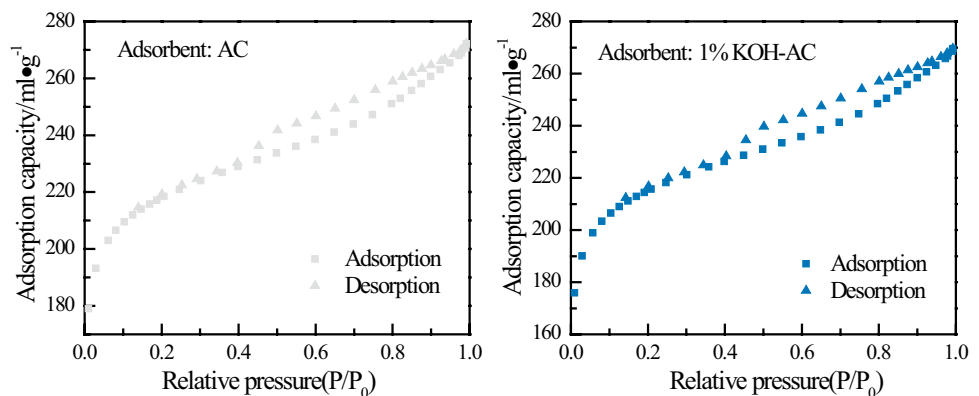


Table 3 Specific surface area and pore volume of coconut shell activated carbon

Adsorbent	S_{BET} (m^2/g)	S_{micro} (m^2/g)	V_{total} (cm^3/g)	V_{micro} (cm^3/g)	V_{meso} (cm^3/g)	V_{macro} (cm^3/g)
AC	711.28	440.77	0.4209	0.1947 (46.26%a)	0.1707 (40.56%b)	0.0557 (13.23%c)
1% KOH-AC	703.42	434.99	0.4170	0.1909 (45.78%a)	0.1731 (41.51%b)	0.0530 (12.71%c)

3350, 3327, and 3229 cm^{-1} . Furthermore, one new characteristic peak of NH was observed at 3485 cm^{-1} . These peaks indicate that the coconut shell activated carbon modified by 1% KOH produces the O–H and N–H on its surface.

3.5 Factor studies on the acetone removal efficiency

Figure 7 shows the effect of the intake time on the average removal efficiency of acetone. The experimental conditions used are the acetone gas concentration of 30.38–42.10 $\mu\text{g}/\text{mL}$ and adsorption temperature at 293 K. With the same intake conditions, 1% KOH-AC shows a better purification effect on acetone than AC. This is caused by O–H functional groups generated on the surface of the coconut shell activated carbon.

The effect of intake airflow on acetone removal efficiency by AC and 1% KOH-AC is shown in Fig. 8. The influence of the intake airflow on the purification effect is evident. When the inlet air flow rate is low with 50 mL/min, acetone's removal efficiency is highest for both AC and 1% KOH-AC. As the inlet flow rate is increased to 100 mL/min, the removal efficiency is reduced, 64.51% for 1% KOH-AC and 46.14% for AC. As the intake airflow continued to increase, the removal efficiency of AC and 1% KOH-AC for acetone decreased significantly. At 250 mL/min airflow, the removal efficiency is decreased, 28.59% for 1% KOH-AC and 19.79% for AC. For the same gas flow rates, 1%

KOH-AC shows better removal efficiency than AC, 20% difference at 100 mL/min.

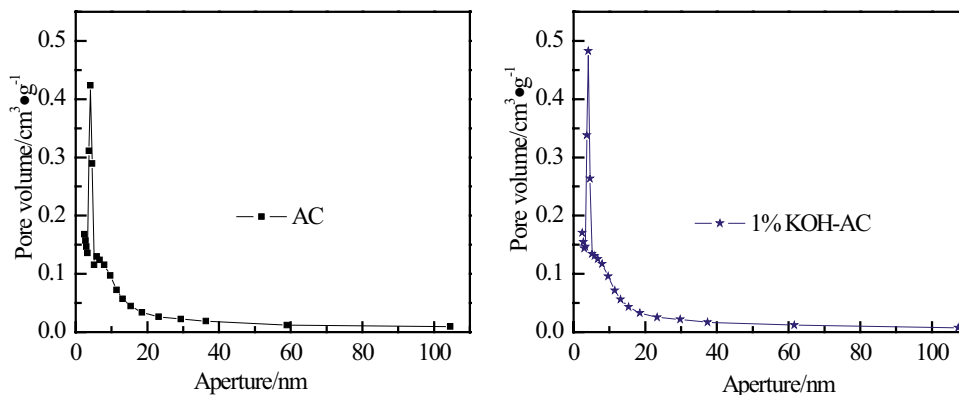
The intake air concentration on acetone's removal efficiency for AC and 1% KOH-AC is shown in Fig. 9. The relationship between the intake air concentration and the removal rate is inversely proportional; as the intake air concentration increases, the removal efficiency decreases.

The effect of the temperature on the adsorption process for acetone purification is shown in Fig. 10. While increasing the temperature of the activated carbon adsorption column from 293 to 303 K, the removal rate of acetone was measured from the activated carbon adsorption column and turned out that its effect was decreased. Consequently, the best temperature for purifying acetone is 293 K. From 293 to 298 K, the removal efficiency of AC to acetone decreased by 3.6% (78.61 to 75.01%) and 7.97% (81.88 to 73.91%) for 1% KOH-AC.

3.6 Adsorption of acetone by AC and 1% KOH-AC

The adsorption isotherms of acetone using two adsorbents of AC and 1% KOH-AC were measured under the conditions of 293 K, 298 K, and 303 K, respectively. The results are shown in Fig. 11.

At $T=293$ K, the adsorption amount of acetone by changing the equilibrium concentrations is measured, and 1% KOH-AC shows 1.2% higher adsorption capacity than AC with 0.88 mg/g and 0.82 mg/g, respectively. At $T=298$ K,

Fig. 5 Distribution of pore volume of coconut shell activated carbon

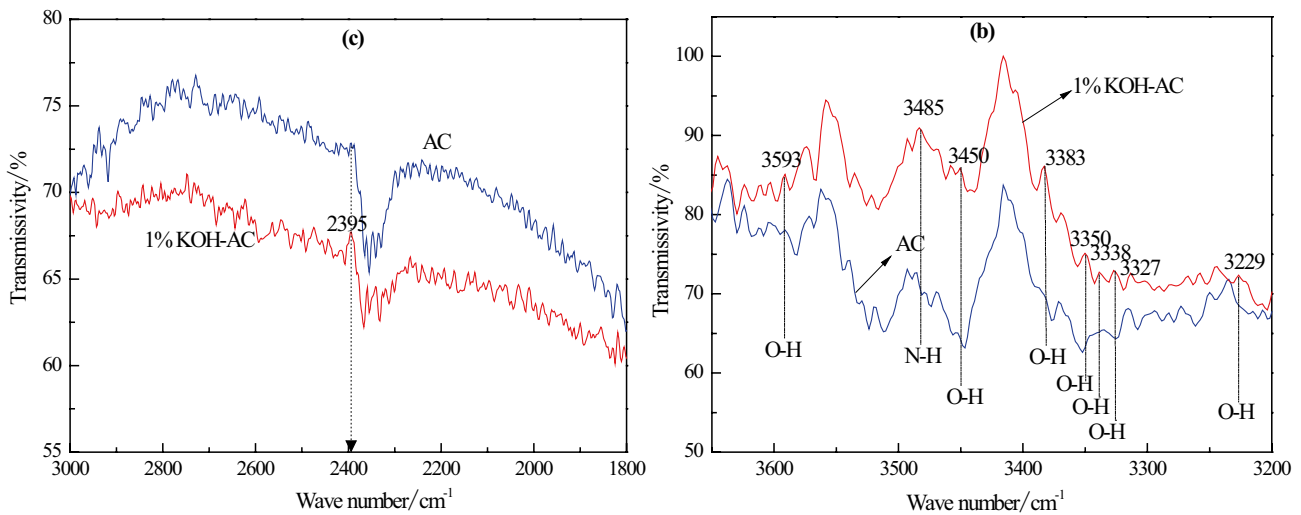


Fig. 6 Fourier transform infrared spectroscopy of coconut shell activated carbon for the wavelength range of 400–4000 cm^{-1} (left), 3200–3700 cm^{-1} (right)

the adsorption amount of acetone by changing the equilibrium concentrations is measured, and 1% KOH-AC shows 17.2% higher adsorption capacity than AC. Moreover, at $T=303\text{ K}$, the adsorption capacity by 1% KOH-AC to acetone is still higher than AC with 25.94%. Therefore, it is concluded that 1% of KOH-AC becomes more significant than AC on acetone’s adsorption as the temperature increases.

3.7 Isotherm model of acetone adsorption by coconut shell activated carbon

The Langmuir adsorption isotherm model and the Freundlich adsorption isotherm model were used to analyzing

acetone’s adsorption by AC and 1% KOH-AC. The Langmuir equation and Freundlich equation were used in curve-fitting for the experimental data shown in Fig. 12, and associated curve-fitting parameters are summarized in Table 4.

The goodness-of-fit test parameter R^2 for the Langmuir model is between 0.986 and 0.998, while R^2 of the Freundlich model that combines the two models is between 0.966 and 0.998. All values of R^2 are more significant than 0.98 and informs of the adsorption of acetone on coconut shell activated carbon as monolayer adsorption.

Because the parameters R^2 of the goodness-of-fit test of the Freundlich model are smaller than the Langmuir model,

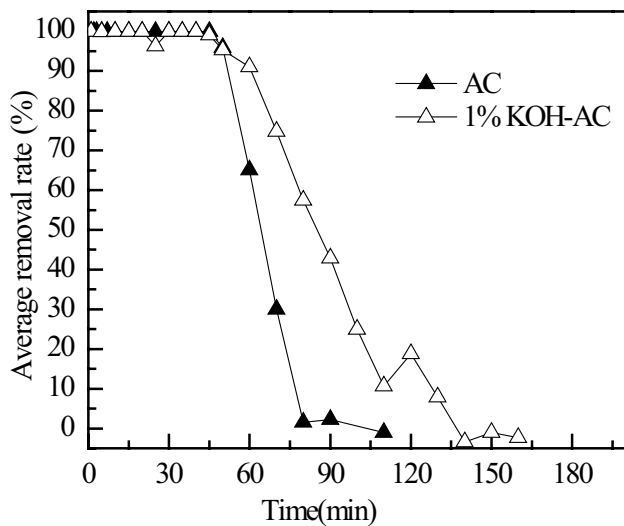


Fig. 7 Effect of intake time on removal efficiency of acetone

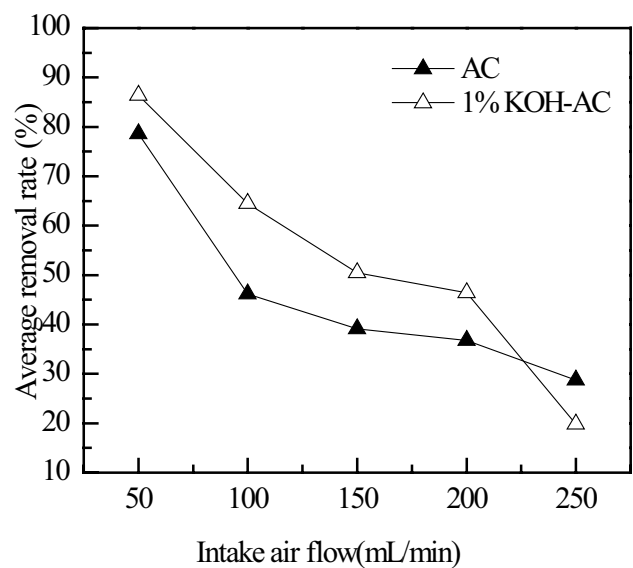


Fig. 8 Effect of intake flow on removal efficiency of acetone

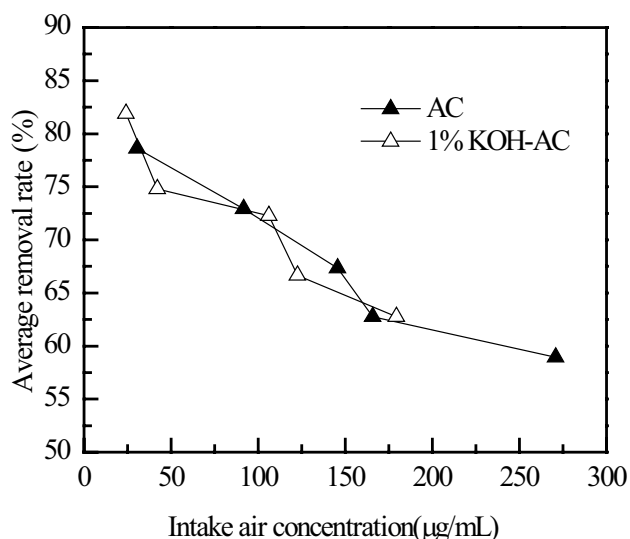


Fig. 9 Effect of imported concentration on removal efficiency of acetone

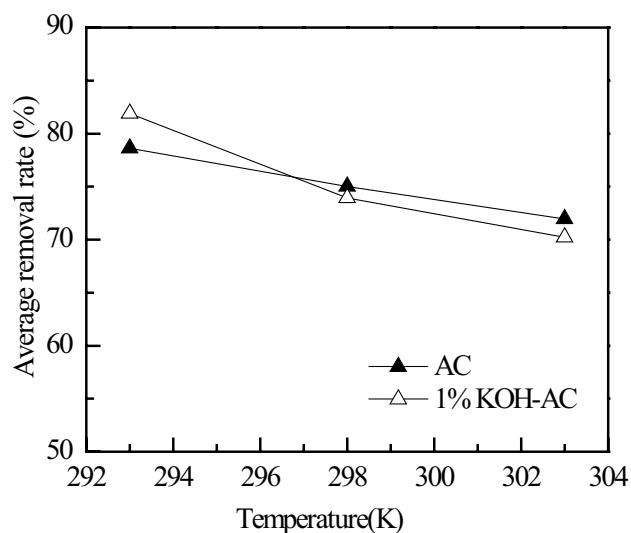


Fig. 10 Effect of adsorption temperature on removal efficiency of acetone

it shows that acetone's adsorption by AC and 1% KOH-AC occurs on a uniform solid surface. By comparing the goodness-of-fit test parameters of the two adsorption models of AC and 1% KOH-AC, it is obtained that the fitting effect of the two models on 1% KOH-AC is better than AC.

3.8 Thermodynamic model for acetone adsorption by coconut shell activated carbon

Using Gibbs' equation and plotting $\ln K$ and $1/T$, ΔH can be obtained from the straight line's slope. Figure 13 is the calculation diagram of the enthalpy change of acetone adsorption by AC and 1% KOH-AC. The corresponding thermodynamic parameters are obtained. The results are shown in Table 5.

According to Table 5, the ΔH of acetone for AC and 1% KOH-AC is -58.70 kJ/mol and -36.97 kJ/mol, respectively, indicating that the adsorption process of acetone on coconut shell activated carbon is an exothermic reaction. The ΔG of AC and 1% KOH-AC adsorption of acetone are negative, indicating that acetone's adsorption on AC and 1% KOH-AC is a spontaneous process and reaction [19]. The negative values of ΔS of AC and 1% KOH-AC for acetone are between $-0.1372 \sim -0.1395$ kJ/mol and $-0.0594 \sim -0.0612$ kJ/mol, indicating that the adsorption is an entropy reduction process, and the system is free. The degree of disorder decreases, and the disorder degree of the solid and air interface decreases.

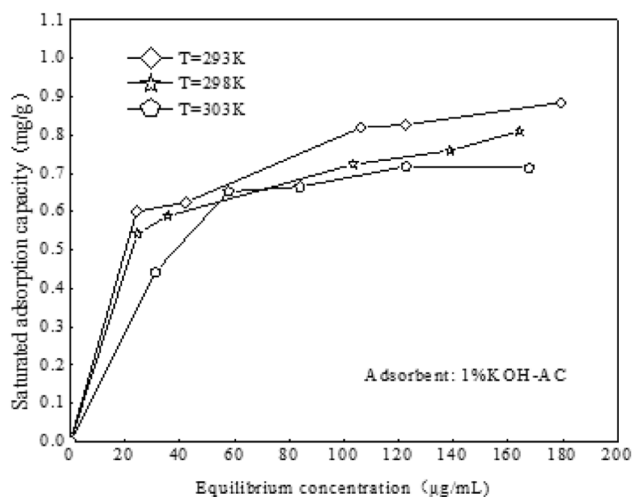
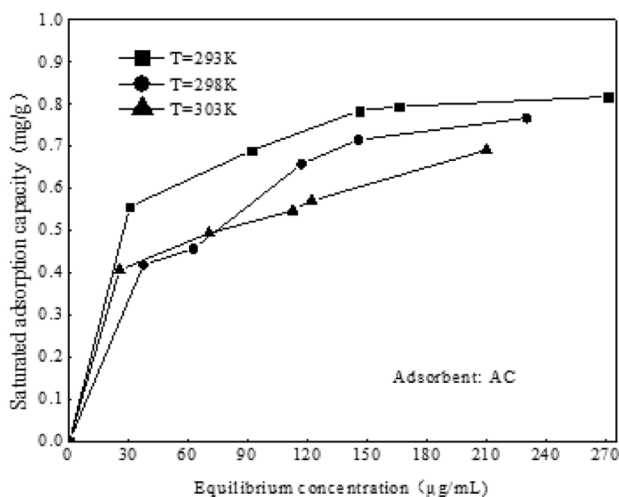


Fig. 11 Adsorption isotherm of acetone on activated carbon at different temperatures

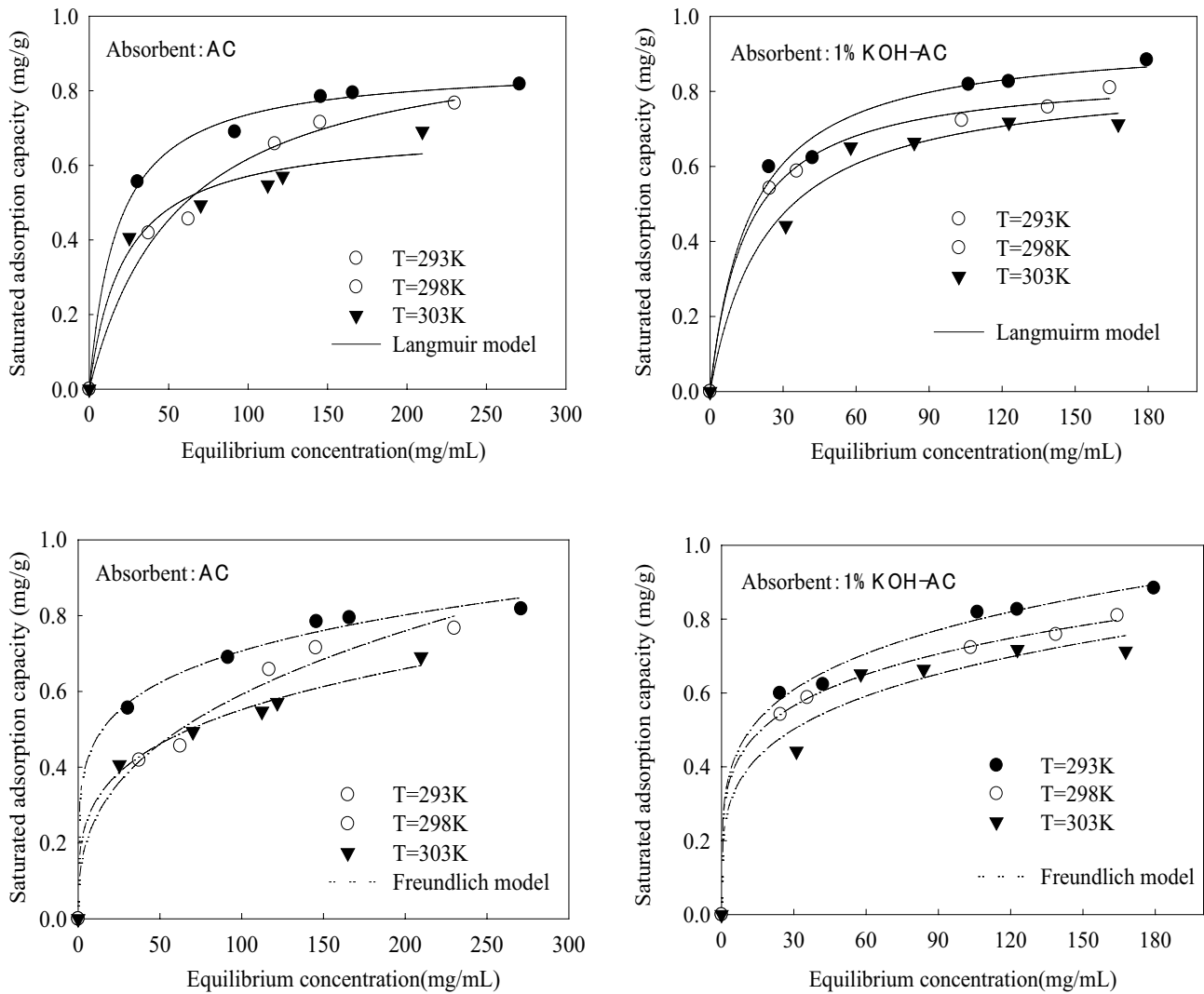


Fig. 12 Isothermal fitting curve of acetone adsorption by activated carbon at different temperatures

3.9 Kinetic model for acetone adsorption by coconut shell activated carbon

In this paper, the quasi-first-order model, quasi-second-order model, Elovich model, and Bangham kinetic model are used to nonlinearly fit the experimental data of AC and 1% KOH-AC adsorption of acetone. The adsorption

temperature is 293 K, 298 K, and 303 K. The change of the adsorption amount on AC and 1% KOH-AC with the intake time is shown in Fig. 14. It can be seen from Fig. 14 that at three temperatures of 293 K, 298 K, and 303 K, the adsorption amount of acetone on AC and 1% KOH-AC increases first and then remains unchanged with the increase of the intake time.

Table 4 Adsorption isotherm fitting parameters of activated carbon to acetone at different temperatures

Adsorbent	T/K	Langmuir model			Freundlich model		
		$K_L/m^3/g$	$q_{max}/mg/g$	R^2	$K_f/m^{3n_f} \cdot mg \cdot g^{n_f} + 1$	n_f	R^2
AC	293	0.0552	0.8694	0.9983	0.3058	0.1819	0.9977
	298	0.0279	0.8372	0.9981	0.17	0.2715	0.9925
	303	0.025	0.6975	0.9864	0.151	0.2795	0.9662
1% KOH-AC	293	0.0698	0.9456	0.9955	0.294	0.2142	0.9983
	298	0.0665	0.8526	0.998	0.2834	0.2028	0.9996
	303	0.0422	0.8458	0.9966	0.2236	0.2377	0.9859

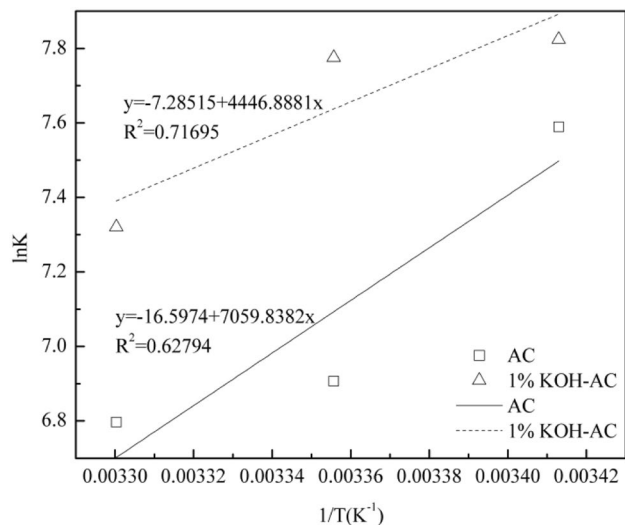


Fig. 13 Calculation of adsorption enthalpy change of acetone adsorbed by AC and 1% KOH-AC

The quasi-first-order kinetic model and quasi-second-order kinetic model for acetone adsorption by AC and 1% KOH-AC at 293 K, 298 K, and 303 K are shown in Table 6.

Table 6 shows that the goodness of fit R^2 of the quasi-first-order kinetic model fits between 0.972 and 0.984. The coefficient of the goodness of fit R^2 of the quasi-second-order kinetic model fits between 0.95 and 0.977. The quasi-first-order dynamic model's model prediction value is closer to the experimental result and has better predictability.

Table 5 Thermodynamic parameters of acetone and 1% KOH-AC adsorption of acetone

Adsorbent	T (K)	ΔH (kJ/mol)	ΔG (kJ/mol)	ΔS (kJ/(mol K))
AC	293	-58.70	-18.49	-0.1372
	298		-17.11	-0.1395
	303		-17.12	-0.1372
1% KOH-AC	293	-36.97	-19.06	-0.0611
	298		-19.26	-0.0594
	303		-18.44	-0.0612

The Elovich model and the Bangham model for acetone adsorption by AC and 1% KOH-AC were fitted at the three adsorption temperatures of 293 K, 298 K, and 303 K. The parameters obtained are shown in Table 7.

Table 7 shows that the goodness of fit coefficient R^2 of the Bangham model fits between 0.996 and 0.997 and higher than those of the Elovich model between 0.920 and 0.971. It indicates that the Bangham kinetic model can describe the kinetics of acetone adsorption by AC and 1% KOH-AC.

From the four kinetic models above, R^2 coefficients are in the order of the Bangham model, the quasi-first-order model, the quasi-second-order model, and the Elovich model. Bangham kinetic model has the best applicability and can better describe acetone's dynamic adsorption process on coconut shell activated carbon.

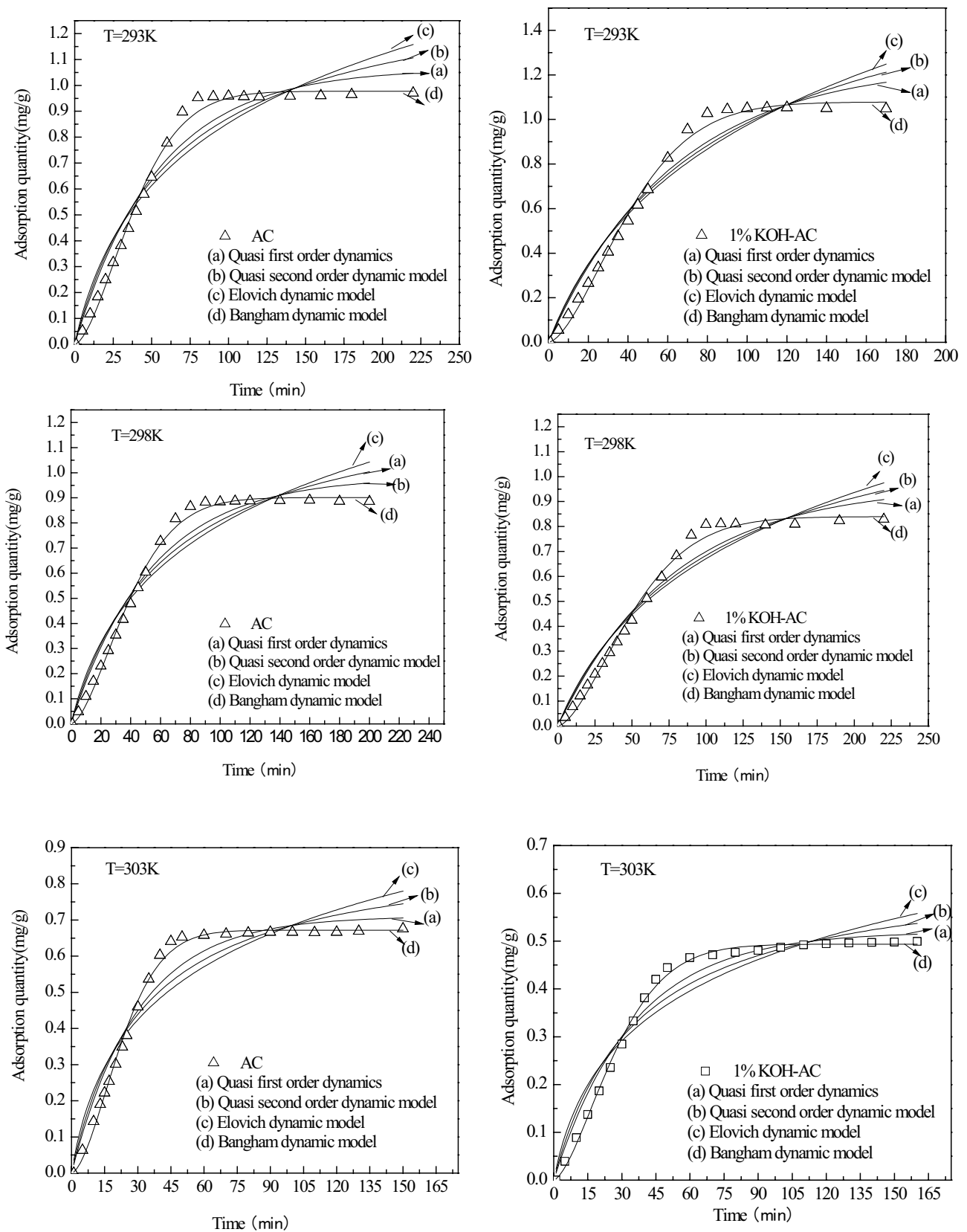


Fig. 14 Fitting curves of four kinetic models for the adsorption of acetone on activated carbon at 293 K, 298 K, and 303 K

Table 6 Pseudo-first-order and pseudo-second-order model fitting parameters of activated carbon adsorption of acetone at different temperatures

Adsorbent	T/K	Quasi-first-order dynamic model			Quasi-second-order dynamic model		
		q_e /mg/g	k_1 /min	R^2	q_e /mg/g	k^2 /g/mg ² /min	R^2
AC	293	0.6986	0.01689	0.97753	1.0631	0.01098	0.97128
	298	0.7474	0.01227	0.98313	0.5640	0.06147	0.97744
	303	0.4573	0.02158	0.98434	0.6458	0.02599	0.97573
1% KOH-AC	293	0.7474	0.01227	0.98313	1.1367	0.00748	0.97744
	298	0.6399	0.02340	0.97248	0.8458	0.02431	0.95370
	303	0.5197	0.02879	0.97295	0.6586	0.04197	0.94983

Table 7 Elovich kinetic model of adsorption of acetone by activated carbon at different temperatures and fitting parameters of Bangham kinetic model

Adsorbent	T/K	Elovich kinetic model			Bangham kinetic model			
		α /mg/g/min	β /g/mg	R^2	k	z	q_e	R^2
AC	293	0.01314	2.5554	0.96521	0.00339	1.5307	0.5749	0.99606
	298	0.02481	6.3531	0.97186	0.00284	1.4539	0.6161	0.99719
	303	0.01212	4.6740	0.96614	0.00526	1.4540	0.4089	0.99900
1% KOH-AC	293	0.01028	2.4048	0.97186	0.00284	1.4539	0.6161	0.99805
	298	0.02148	4.0302	0.93235	0.00383	1.5373	0.5971	0.99682
	303	0.02454	5.6286	0.92007	0.00463	1.5558	0.4938	0.99721

4 Conclusion

This research discusses and presents acetone's adsorption as an organic waste gas by modified coconut shell activated carbon. One percent KOH was selected as the modifier for coconut shell activated carbon after exhibiting the best performance. The determination of acetone removal efficiency and adsorption amount of coconut shell activated carbon before and after modification shows that the removal efficiency of coconut shell activated carbon to acetone first reaches 100%, then decreases with the increase of intake time. It was also found that the removal of acetone is affected by the temperature; the lower the adsorption temperature, the easier it is to remove acetone. When used on the same exhaust gas, the removal ability of 1% KOH-AC is stronger than AC. The adsorption amount of acetone from coconut shell activated carbon initially increased then remained unchanged with equilibrium concentration.

Furthermore, it was found that the equilibrium adsorption amount of acetone from 1% KOH-AC was higher than AC, and the adsorption process of acetone from coconut shell activated carbon was exothermic. The coconut shell-activated carbon characterization results, such as thermodynamics and kinetic experiments, verify that AC and 1% KOH-AC are mesoporous and microporous activated carbon structures. Their specific surface areas are in order of AC, 1% KOH-AC. Besides, the functional groups on the surface of the modified coconut shell activated carbon presented significant alterations. One percent KOH-AC showed characteristic O–H peaks at 3485 cm⁻¹ wave

number and characteristic peaks of N–H at 3229 cm⁻¹ wave number. The Langmuir model can better predict the adsorption isotherm of acetone on coconut shell activated carbon. The adsorption of acetone on coconut shell activated carbon is single molecular layer adsorption, and the adsorption occurs on a uniform solid surface. There are two adsorption models for 1% KOH-AC. The fitting effect is better than AC. The ability of 1% KOH-AC to adsorb acetone is stronger than AC. Thermodynamic experiments show that AC and 1% KOH-AC's adsorption reaction to acetone is a spontaneous exothermic reaction. The increase in temperature is not conducive to adsorption. Moreover, the progress of the response for both types of adsorption is entropy reduction processes. The fitting goodness test parameter R^2 of the Bangham model is the highest, proving that the Bangham model has a higher fitting degree of equilibrium adsorption.

Acknowledgements We thank the Yunnan Innovative Research Team of Environmental pollution, Food Safety and Human Health for granting the technical guidance toward this research work.

Funding Partial support of the present study by the Open fund of Key Laboratory of Ecological Environment Evolution and Pollution Control in Mountainous Rural Areas of Yunnan Province (Project Nos. 2020YB006), Key Laboratory of State Forestry and Grassland Administration on Highly-Efficient Utilization of Forestry Biomass Resources in Southwest China, Southwest Forestry University (Project Nos. 2020YB006), Scientific research fund of Yunnan Education Department (Project Nos. YB202023), Science popularization project of philosophy and Social Sciences Planning of Yunnan Province in 2021 (SKPJ202121) and Scientific research fund project of Yunnan Education Department (Project Nos. 2021J0163).

Declarations

Conflict of interest The authors declare no competing interests.

References

1. Tong R, Ma X, Zhang Y, Shao G, Shi M (2020) Source analysis and health risk-assessment of ambient volatile organic compounds in automobile manufacturing processes. *Hum Ecol Risk Assess Int J* 26:359–383. <https://doi.org/10.1080/10807039.2018.1510729>
2. Huang Y et al (2020) Competitive adsorption of benzene and water vapor on lignite-based activated carbon: Experiment and molecular simulation study. *Chem Eng J* 398:125557. <https://doi.org/10.1016/j.cej.2020.125557>
3. Jung SC et al (2019) Catalytic Performance of supported Pd catalyst prepared with different palladium precursors for catalytic combustion of BTH. *J Nanosci Nanotechnol* 19:1208–1212. <https://doi.org/10.1166/jnn.2019.15950>
4. Lebrero R, Volckaert D, Pérez R, Muñoz R, Van Langenhove H (2013) A membrane bioreactor for the simultaneous treatment of acetone, toluene, limonene and hexane at trace level concentrations. *Water Res* 47:2199–2212. <https://doi.org/10.1016/j.watres.2013.01.041>
5. Gales L, Mendes A, Costa C (2002) Removal of acetone, ethyl acetate and ethanol vapors from air using a hollow fiber PDMS membrane module. *J Membr Sci* 197:211–222. [https://doi.org/10.1016/S0376-7388\(01\)00628-7](https://doi.org/10.1016/S0376-7388(01)00628-7)
6. Lee S-W, Na Y-S, An C-D, Lee M-G (2012) Comparison of adsorption and desorption characteristics of acetone vapor and toluene vapor on activated carbons according to pore structure. *J Environ Sci* 21:1195–1202. <https://doi.org/10.5322/JES.2012.21.10.1195>
7. Yuan H et al (2020) Photodegradation of gaseous toluene by vacuum ultraviolet light: performance and mechanism. *Eng Sci* 9:68–76. <https://doi.org/10.30919/es8d910>
8. Deng Z et al (2021) Modifying coconut shell activated carbon for improved purification of benzene from volatile organic waste gas. *Adv Compos Mater*. <https://doi.org/10.1007/s42114-021-00273-6>
9. Deng Z et al (2021) Modification of coconut shell-based activated carbon and purification of waste water. *Adv Compos Mater* 4:65–73. <https://doi.org/10.1007/s42114-021-00205-4>
10. Di M et al (2021) Preparation of selenium-rich tea set and its release properties of selenium in water. *ES Mater Manuf* 13:89–96. <https://doi.org/10.30919/esmm5f435>
11. Pan D, Su F, Liu C, Guo Z (2020) Research progress for plastic waste management and manufacture of value-added products. *Adv Compos Mater* 3:443–461. <https://doi.org/10.1007/s42114-020-00190-0>
12. Gallego E, Roca FJ, Perales JF, Guardino X (2013) Experimental evaluation of VOC removal efficiency of a coconut shell activated carbon filter for indoor air quality enhancement. *Build Environ* 67:14–25. <https://doi.org/10.1016/j.buildenv.2013.05.003>
13. Sun Z et al (2021) Corn-cob-derived activated carbon for efficiently adsorption dye in sewage. *ES FAF* 4:61–73. <https://doi.org/10.30919/esfaf473>
14. Mao H et al (2016) Adsorption of toluene and acetone vapors on microwave-prepared activated carbon from agricultural residues: isotherms, kinetics, and thermodynamics studies. *Res Chem Intermed* 42:3359–3371. <https://doi.org/10.1007/s11164-015-2217-9>
15. Kang KH, Lee MG (2018) Adsorption characteristics of acetone, benzene, and methylmercaptan in the fixed bed reactor packed with activated carbon prepared from waste citrus peel. *Appl Chem Eng* 29:28–36. <https://doi.org/10.14478/ace.2017.1094>
16. Marahel F, Ghaedi M, Ansari A (2015) Zinc oxide nanoparticles loaded on activated carbon and its application for adsorption removal of uric acid. *Synth React Inorg, Met-Org, Nano-Met Chem* 45:1387–1395. <https://doi.org/10.1080/15533174.2013.862657>
17. Tovar-Gómez R et al (2015) Analysis of synergistic and antagonistic adsorption of heavy metals and acid blue 25 on activated carbon from ternary systems. *Chem Eng Res Des* 93:755–772. <https://doi.org/10.1016/j.cherd.2014.07.012>
18. Kayan A (2019) Inorganic-organic hybrid materials and their adsorbent properties. *Adv Compos Mater* 2:34–45. <https://doi.org/10.1007/s42114-018-0073-y>
19. Jiao Y et al (2011) Identifying a major locus that regulates spontaneous arthritis in IL-1ra-deficient mice and analysis of potential candidates. *Genet Res (Camb)* 93:95–103. <https://doi.org/10.1017/S0016672310000704>

Publisher's Note Springer Nature remains neutral with regard to jurisdictional claims in published maps and institutional affiliations.